Modeling Interdependencies Between the Building Portfolio, Transportation Network, and Healthcare System in Community Resilience

Omar A. Sediek[1], Sherif El-Tawil[2], and Jason McCormick[3]

ABSTRACT

A community resilience model that takes into account the mutual interdependencies between the building portfolio, transportation network, and healthcare system both during and after a seismic event is presented. The model is modularized into independent simulators to facilitate modeling their interdependencies. The transportation network model accounts for the capacity reduction attributed to bridge damage and links blocked by debris from collapsed buildings. It also addresses the increased demand from ambulance trips ferrying injured people to healthcare facilities and trucks hauling away debris. The transportation network model is incorporated into a discrete event simulation environment that models the response of the healthcare system as well as the debris removal process in the aftermath of a seismic event. Measures are proposed to quantify and improve the seismic resilience of each individual system as well as the whole community considering the three systems' mutual interdependencies. The capability of the proposed model to support hazard mitigation planning is demonstrated through a case study that highlights the effects of interdependencies between the three systems under consideration. Mitigation strategies to improve seismic resilience of a prototype community are proposed and assessed.

---

[1]Ph.D. Candidate, Department of Civil & Environmental Engineering, University of Michigan, Ann Arbor, MI 48109-2125; email: osediek@umich.edu
[2]Professor, Department of Civil & Environmental Engineering, University of Michigan, Ann Arbor, MI 48109-2125; email: eltawil@umich.edu
[3]Professor, Department of Civil & Environmental Engineering, University of Michigan, Ann Arbor, MI 48109-2125; email: jpmccorm@umich.edu

INTRODUCTION

Severe earthquakes generate complex interactions between the building portfolio, transportation network and healthcare system of a community. The interdependencies between the three systems profoundly influence first response activities and extend into the long-term recovery effort. Building collapse produces debris piles that may block or reduce the capacity of adjacent roadways, thereby impairing the capacity of the transportation network. The transportation network's capacity may be further compromised by seismic damage to the bridges within the network. The healthcare system, which itself may see damage to its buildings during a seismic event and hence has a reduced capacity, contributes traffic to the impaired transportation network in the form of ambulance trips. Post-earthquake casualties in the community affect the availability of the workforce (i.e., construction labor) in the community, which in turn affects the recovery of the building portfolio. The effort to haul away debris piles places additional demands on the transportation network, which at the same time, is called upon to also handle day-to-day traffic as the community strives to recover from the disruption. These complex interactions are shown in Figure 1.

Previous studies have focused on the behavior of one of these infrastructure systems. For example, Burton et al. (2017), Gentile and Galasso (2020) and Fu et al. (2021) studied the response of the building portfolio. Kirsch et al. (2010), Mitrani-Reiser et al. (2012), and Hassan and Mahmoud (2020) focused on the response of the healthcare system, while Vishnu et al. (2018), Zhang et al. (2019) and Somy et al. (2021) analyzed the transportation network.

Moving away from a focus on a single system, some studies have investigated the effect of the seismic debris field generated by damaged structures on the transportation network, e.g., Hirokawa and Osaragi (2016), Castro et al. (2019), and Feng et al. (2020). These studies used empirical approaches for modeling the debris field. A more rational approach for modeling the debris field can be found in Domaneschi et al. (2019) and Sediek et al. (2021a) who used a computational technique, the Applied Element Method (AEM), to model building collapse and the extent of the debris piles. However, Domaneschi et al. (2019) and Sediek

et al. (2021a) did not explicitly consider the interdependency between the building system and transportation network.

Buildings that collapse or are damaged during seismic events are no longer able to provide their intended service. Sediek et al. (2020) mapped the damage of the components of the buildings to their post-earthquake functionality. A reduced post-earthquake functionality of buildings affects the origin-destination (O-D) travel patterns since community residents who use those buildings as homes or for work will not travel to or from these locations. Shiraki et al. (2007) related the O-D reduction rates to the seismic intensity of the event. However, use of a constant reduction rate is not realistic because the level of building damage, and hence functionality loss, can greatly vary across the community.

The effect of post-earthquake traffic (i.e., travel time) on the transportation network controls the number of ambulance trips that can be made. Fawcett and Oliveira (2000) proposed a regional simulation model for casualty treatment after earthquake disasters. In their model, they used the pre-earthquake travel times between all pairs of zones in the community to estimate the number of injuries that can be mobilized in each time interval. However, travel times can be impacted by the state of the transportation network. Ceferino et al. (2020) proposed a methodology to evaluate emergency response of the healthcare system based on a model that assesses the loss of hospital functionality and quantifies multi-severity injuries (i.e., injuries with different levels of severity) as a result of earthquake damage. However, their model did not consider the effect of the transportation network on the healthcare system.

Unlike the Fawcett and Oliveira (2000) and Ceferino et al. (2020) studies, Cimellaro et al. (2013) used agent-based models to evaluate the functionality and resilience of healthcare facilities after seismic events taking into account the functionality of the roadway system. While the Cimellaro et al. (2013) study went farther than others by considering the condition of the roadway system on the healthcare system, it did not consider the opposite effect, i.e., the effect of the healthcare system on the transportation network. The trips

made by ambulances in the first few days after the earthquake between the locations of the injured and the hospitals in the community affects the travel time and flow on the links of the transportation network.

Based on the studies surveyed above, there are key limitations in the available models for assessing community resilience especially when dealing with mutual interdependencies between the infrastructure systems shown in Figure 1. Given these limitations and the dearth of research results, this paper proposes a new multidisciplinary simulation model that focuses on modeling the mutual interdependencies outlined in Figure 1 between the building portfolio, transportation network, and healthcare system in a community.

The proposed model simulates the capacity of the transportation network as a function of the combined effect of bridge damage and the accumulation of debris resulting from the collapse of buildings. The transportation network model is then incorporated into a discrete event simulation environment that accounts for the response of the healthcare system as well as the debris removal process to model the aftermath of a seismic event. The capability of the proposed model to support hazard mitigation planning is demonstrated through a case study that highlights the mutual interdependencies between the three studied systems.

SIMULATION MODEL OVERVIEW

Figure 2 shows an overview of the proposed simulation model. The modular design implemented by Sediek et al. (2020) is used to connect the models (termed simulators) representing different aspects of the community. As shown in Figure 2, each of the simulated systems (i.e., building portfolio, transportation network, and healthcare system) is represented by a set of simulators. The ability to account for the interdependencies between the different systems is achieved through the connection between the individual simulators. The simulators are connected through two types of connections: sequential and interdependent as shown in Figure 2. Sequential connection implies that the latter simulator is dependent on the former one, whereas interdependent connection implies that both simulators are mutually dependent.

The proposed simulation model runs in four stages, each with a different time scale. The model starts with the pre-earthquake stage where the community setup is loaded and broadcast to all the simulators in the simulation model through the *city* simulator. The pre-earthquake behavior of the transportation network is evaluated in the *pre-earthquake traffic* simulator. The second stage is during the earthquake, where the time step is taken in seconds After the earthquake, there is a transition stage where the *bridge* and *building downtime* simulators are executed in a single step to evaluate seismic losses. The final stage is the recovery stage, where the time step is taken in days in all the simulators except for the *healthcare* and *post-earthquake traffic* simulators. For the *healthcare* simulator, the time step is taken in hours (i.e., 2 hours for each time step) to rigorously simulate the emergency response of the healthcare system in the community after the earthquake, as will be discussed later. For the *post-earthquake traffic* simulator, the time step is taken as 10 days after the first 30 days as discussed later. During the recovery stage, the recovery trajectory of the different systems in the community is evaluated with explicit modeling of the interdependencies between them.

More details about the implementation of the *city*, *ground motion*, *structural analysis*, *building damage*, *component damage*, *casualties*, *buildings downtime*, *building recovery*, and *available resources* simulators can be found in Sediek et al. (2020). The implementation of the *pre-earthquake traffic*, *debris, bridge damage, bridge downtime*, *bridge recovery*, *healthcare*, *debris removal*, *post-earthquake traffic*, and *network recovery* simulators is discussed later.

METHODOLOGY

Pre-Earthquake Traffic Simulation

As shown in Figure 2, the *pre-earthquake traffic* simulator receives information about the transportation network in the community under consideration from the *city* simulator. Transportation networks usually are comprised of two main components: roads and bridges. These networks are often represented

mathematically using graph theory (Biggs et al. 1986). In graph theory, a network is represented by vertices (called nodes) connected together using edges (called links). In transportation networks, the nodes represent the intersection between the roads whereas the links are the roadways between these nodes. The level of detail included in the modeled transportation network (i.e., links represent only highways or every road in the region) depends on the available computational resources and the purpose of the simulation. Information about the transportation networks in the U.S. and around the world (i.e., node locations, links connecting nodes, capacity and maximum speed on roads, etc.) is publicly available in many open-source platforms (e.g., OpenStreetMap, OSM).

The normal pre-earthquake traffic conditions of the transportation network (i.e., travel time, flow on links, and route choice of each vehicle) are evaluated in the *pre-earthquake traffic* simulator using a four-step model which has been developed and widely used since the 1950s (see Weiner 1997). The four steps are: trip generation, trip distribution, mode choice, and route assignment. Before applying the four-step model, the studied community is divided into smaller traffic analysis zones (TAZ). TAZs are geographic areas with relatively similar land use and activity. They represent the origins and destinations of travel activity within the studied community. Trip generation is performed to predict the trip productions and attractions between the different TAZs for different purposes (i.e., home-based, work-based, etc.). A cross-classification model is adopted in the present study because it is based on data from real cities (e.g., the travel demand model used by Memphis Urban Area Metropolitan Planning Organization [MPO]).

Trip distribution is performed to distribute the predicted production and attractions between the different TAZs as origin-destination (O-D) pairs. A widely used gravity model (Isard 1956), based on Newton's Theory of Gravity, is adopted to perform this step. Mode choice is performed to distribute the O-D pairs between the different modes of transportation available in the city (i.e., vehicles, bus, bike, etc.). A trip end model is adopted to perform this step in the current study based on data from real cities. The final step in the four-step model is route assignment which uses the O-D pairs developed by the mode choice step to

assign the routes for each O-D pair based on the state of the transportation network (i.e., capacity and maximum speed of the links in the network). The most widely used method to perform this step is the static user equilibrium (UE) model proposed by Evans (1976) which is used herein. In this methodology, the transportation network is assumed to reach equilibrium when the cost of travel (i.e., travel time) on any route for any traveler in the O-D pair cannot be improved by choosing another route (Wardrop 1952).

Debris Generation

The *debris* simulator receives the damage state of each structural and nonstructural component in the building from the *building* and *component damage* simulators to characterize the seismic debris field in the community. As outlined in Sediek et al. (2021a), the seismic debris is characterized by two attributes: quantity and extent. The debris quantity is the amount of debris generated in tons, whereas the debris extent is the size of the footprint of the debris field around the damaged building. In the current study, the debris quantity is estimated using the methodology described in HAZUS (FEMA 2003).

The extent of debris generated from the collapse of each building in the community is evaluated based on its type (i.e., RC, steel, ...etc.) using different approaches as summarized in Figure 3. For RC frame buildings, the approach developed by Sediek et al. (2021a) is adopted. In this approach, the seismic debris field is characterized using three types of data: (1) mode of collapse, (2) collapse direction, and (3) debris extent. The mode of collapse of the building is predicted using a deep neural network (DNN) based on the input ground motion and building height. Modes 1 and 2 are classified as aligned modes (aligned with one of the building's axes), whereas modes 3 and 4 are classified as skewed modes as shown in Figure 3(a). The collapse direction is predicted using a uniformly distributed random number. As shown in Figure 3(a), the debris footprint is larger than the original footprint by the dimensions a, b, c, and d, where a is always assigned the largest dimension. These four dimensions are estimated probabilistically using the 3D lognormal distribution fit by Sediek et al. (2021a). The parameters of the fitted distributions are listed in Table 1 for different modes of collapse and building heights.

For masonry buildings, the approach developed by Domaneschi et al. (2019) is adopted. In this approach, the area of the seismic debris field is assumed to be larger than the original building area by an amplification factor, ε, as shown in Figure 3(b). The amplification factor is evaluated as:

$$\varepsilon = 1.228 + 0.0787\left(\frac{L}{W}\right) + 0.0563\left(\frac{A_f h_b^2}{V_b L}\right) \quad (1)$$

where L and W are the building length and width, respectively, A_f is the footprint area of the building, h_b is the building height, and V_b is the total masonry volume of the building.

For other types of buildings in the community, the debris around the collapsed building is assumed to form a triangular prism with the long side adjacent to the collapsed building as shown in Figure 3(c) (Argyroudis et al. 2015). Per Argyroudis et al. (2015), the width of debris outside the building envelope (W_d) is evaluated as:

$$W_d = \sqrt{W^2 + \frac{2k_v WH}{\tan\theta}} - W \quad (2)$$

where W is building width perpendicular to the road's axis, k_v is the proportion of the volume of debris with respect to the original volume, and θ is the angle of collapse. k_v and θ are assumed to be statistically independent random variables with normal distribution, where: $\mu_{kv} = 0.5$, $\sigma_{kv} = 0.15$, $\mu_\theta = 45^o$, and $\sigma_\theta = 13.5^o$ (Argyroudis et al. 2015). For all buildings, the percentage of roadway blockage adjacent to the collapsed buildings due to seismic debris is estimated by subtracting the building setback from the debris extent in the direction of the roadway.

Bridge Damage and Recovery

The *bridge damage* simulator receives the ground motion parameters from the *ground motion* simulator to evaluate the damage state of each bridge in the transportation network based on the fragility curves specified in HAZUS (FEMA 2003). Five damage states are differentiated in HAZUS: no damage, slight, moderate,

extensive, and complete damage. Two types of links are attached to each bridge in the network: major and minor links. Major links are those links that are directly connected to and affected by damage to a bridge. Minor links are those links that are indirectly connected to and affected by damage to a bridge (i.e., the roadway under the bridge). For a major link, it is assumed that any damage to the bridge will cause complete closure of that link. For a minor link, only extensive and complete damage to the bridge are assumed to cause complete closure of that link based on the definition of extensive and complete damage states in HAZUS (FEMA 2003).

The recovery process of the bridge is assumed to be discrete as per Padgett and DesRoches (2007) where the bridges are assumed to open when they reach either partial (e.g., 50%) or full (100%) functionality. Thus, three levels of bridge functionality are differentiated: closed (0%), partially open (50%), and open (100%). The partial functionality (i.e., 50%) of the bridge is interpreted as half capacity with a free flow speed of the major link attached to the bridge in the pre-earthquake condition. The repair time for these levels of functionality is taken as per Padgett and DesRoches (2007).

Post-Earthquake Traffic Simulation

The travel time and flow on each link in the transportation network are evaluated in the *post-earthquake traffic* simulator based on the updated conditions of the transportation network. The *post-earthquake traffic* simulator runs once every 10 time steps (i.e., 10 days) after the first 30 days during the recovery stage as discussed earlier due to the computational cost of the traffic analysis. It is assumed that the behavior of the transportation network is constant between these time steps after the first 30 days. During the first 30 days, the *post-earthquake traffic* simulator runs each time step to rigorously model the post-earthquake emergency response of the community. The 30-day threshold is chosen based on the emergency response of real communities against historical seismic events (e.g., Bruycker et al. 1983).

The four-step model is adopted once again to perform the traffic analysis. The second and third steps in the model (i.e., trip distribution and modal split) are assumed to be the same as before the seismic event. However, the first and fourth steps are updated to consider the effect of the seismic event and the interdependencies discussed earlier. The trip productions and attractions between the TAZs are reduced based on the reduction in the functionality of each building in the TAZ. The reduction values are adopted from Sediek et al. (2020) based on the functionality state of each building (i.e., not functional, re-occupancy, basic functionality, and full functionality).

A mutual interdependency that has not been previously studied in any significant depth but is considered in the current study is the interaction between the *healthcare* and the *post-earthquake traffic* simulators (see Figure 1 and Figure 2). The trips made by ambulances between the locations of injured people (i.e., produced) and hospitals in the community (i.e., attracted) and vice versa are added to the productions and attractions in the trip generation step. Another mutual interdependency exists between the *debris removal* and the *post-earthquake traffic* simulators (see Figure 2). The trips made by trucks to remove the generated debris from the locations of building collapse (i.e., produced) to the debris management sites and final disposal locations (i.e., attracted) and vice versa are also added to the productions and attractions in the trip generation step.

Route assignment is performed using the static user equilibrium (UE) model discussed earlier. However, the capacity and free flow speed of each link in the network are updated based on the bridge functionality and extent of debris that encroaches onto surrounding roadways. The reduction of the capacity and free flow speed of a link in the transportation network is assumed to be the maximum of the reduction due to bridge damage and debris extent. The reduction due to debris extent on a link is assumed to be the maximum percentage of road blockage due to seismic debris generated from all the collapsed buildings adjacent to that link. The reduction due to bridge damage is assumed to be the maximum reduction in functionality of all the bridges attached to a link. Both reductions are updated each time step during the recovery stage as

the debris is removed and bridges recover. The dynamic nature of the simulation model allows straightforward consideration of such complex interdependencies.

Discrete-Event Simulation of Healthcare System

Discrete-event simulation (DES) is the process of modeling the behavior of complex systems using an ordered sequence of well-defined events (Robinson 2004). It can be used to study what-if scenarios by changing the input parameters of the simulation and studying the effect of these changes on the modeled system. It has been widely used over the past decade to simulate the behavior of various engineering (e.g., Alvanchi et al. 2011), economic (e.g., Cigolini et al. 2014), and healthcare systems (e.g., Jun et al. 1999, Hamrock et al. 2003, and Hasan et al. 2020). In the present study, DES is used to model the behavior of the healthcare system during the post-earthquake stage. A fixed-increment time progression scheme is adopted where the time after the earthquake is divided into small equal intervals of two hours each and the state of the healthcare system is updated each time interval depending on the events occurring in this time interval.

The *healthcare* simulator runs for the first 360 hours (i.e., 15 days) for a total of 180 time intervals. Figure 4 shows a schematic diagram for the DES implemented in the *healthcare* simulator. As shown, the simulation is separated spatially into two locations (i.e., the injuries are assumed to be in one of two locations): traffic analysis zones (TAZs) or hospitals. First, the number of injuries and fatalities in each TAZ is evaluated during the earthquake stage in the *casualties* simulator. It is assumed that 60% of the injuries in TAZs are trapped inside buildings and need to be rescued during the recovery stage as per Facwett and Oleveria (2000). The rescue rate in each time interval is assumed to follow an exponential decay function (i.e., Ae^{-Bt}) defined by parameters A and B that depend on the emergency response capabilities of the studied community, where t is the time after earthquake.

The other 40% are transported to the hospitals in the community during the recovery stage based on the availability of ambulances and beds in the hospitals. The ambulances are distributed among the hospitals

based on the availability of beds in each hospital which is evaluated in the *physical recovery* simulator. The ambulances are distributed among TAZs based on the smallest travel time on the transportation network. The number of injuries that can be mobilized between the TAZs and hospitals using a specific ambulance in a certain time interval depends on the travel time on the transportation network subscribed from the *post-earthquake traffic* simulator and the loading and unloading times of the injured into and out of the ambulances. The loading and unloading times are assumed to be random variables having a triangular (4.36,1.8) + 0.83 minutes and lognormal distributions (-0.49,3.36,5.54) minutes, respectively as per Su et al. (2008).

The admission of the injuries to the hospital depends on the number of beds available in the hospital. Previous earthquakes showed that multiple patients can occupy the space allocated to one bed during post-earthquake emergencies in real hospitals. For example, after the M_w 7.8 Kashmir earthquake, Mulvey et al. (2008) reported that up to 4 patients on average occupied the space allocated for one bed during the first 72 hours in a military hospital in the Forward Kahuta town. Therefore, a multiplier of 4 is assumed for the number of patients that can be admitted to hospitals during the post-earthquake stage. The total number of beds available at any time in the hospital is proportional to the physical functionality of the hospital (Sediek et al. 2020) as well as the social functionality of the medical staff in the hospital which is assumed proportional to the number of injuries in the community (i.e., the percentage of injuries in the medical staff is assumed the same as the percentage of injuries in the population of the community). Based on Sediek et al. (2020), it is also assumed that 5% of the injuries waiting admission to hospitals or waiting mobilization from TAZs each time step (i.e., 2 hours) are taken to a hospital beyond the study region using resources outside the considered community.

The length of stay of an injured person in a hospital is assumed to be a random variable with lognormal distribution having a median of 3 days, dispersion of 0.4 and maximum of 64 days as was observed after the M_w 7.7 2001 Gujarat earthquake (Phalkey et al. 2011). During the first days after the earthquake, there

is a high mortality rate which is about 20-25 % according to Coupland (1994). The proposed simulation model considers a variable mortality rate for untreated injuries based on where the injured person is located (i.e., trapped inside a collapsed building or waiting admission to the hospital) and the number of days after the earthquake as listed in Table 2.

Discrete-Event Simulation of Debris Removal

Debris removal is generally performed in two stages: (1) clearing emergency routes to expedite rescue operations; and (2) clearing remaining roadways as a means to recovery (FEMA 325 2007). The transition between stage 1 and stage 2 depends on the impact of the seismic debris on the road network as well as the number of trapped people after an earthquake. FEMA-325 (2007) classifies seismic debris into: construction and demolition debris; white goods; hazardous waste; and soil, mud, and sand. Generally, specific procedures are required to remove each debris type. However, FEMA-325 (2007) proposes a general framework for all types of debris as shown in Figure 5. The debris is first collected from the building's location to a temporary debris management site (TDMS), where it is sorted, reduced, and recycled before transportation to its final disposal landfill. The location of the TDMS in the community is ideally predefined before the earthquake based on the specifications suggested by the US EPA (U.S. Environmental Protection Agency) and UNEP (United Nation Environment Program). It should be located near the impacted area of the community but away from residential and commercial neighborhoods. The optimal choice of TDMS is an open research question that has been rarely studied (Kim et al. 2018) and outside the scope of the current study.

In the *debris removal* simulator, DES is used to simulate the process of debris removal from TAZs to TDMSs and then to landfills (LFs) during the post-earthquake stage. Similar to the healthcare system, a fixed-increment time progression scheme is adopted where the time after the earthquake is divided into small equal intervals of one day each. The *debris removal* simulator runs for the first 365 days (i.e., 1 year) after the earthquake. Figure 6 shows a schematic diagram for the DES implemented in the *debris removal*

simulator. As shown, the trucks in the community are distributed to transport the debris from the building locations (i.e., TAZs) to TDMSs or from TDMSs to LFs or from TDMSs to recycling facilities in the community. The number of trucks assigned to each task is a decision parameter that can be optimized to enhance the performance of the debris removal system in the community. First, the amount of debris (in tons) evaluated by the *debris* simulator at the location of each building is converted into cubic yards (CY) using a factor of 2 as specified by FEMA (2010) for construction and demolition debris.

The trucks used to transport the debris from the buildings to TDMSs are distributed among the TDMSs based on the available space in the TDMSs. It is assumed that the capacity of each TDMS is 30,000 CY as per Kim et al. (2018). The number and locations of TDMSs in the community is an input parameter to the proposed model and can be optimized to enhance the performance of the debris removal process. The debris is collected from the building locations based on the importance of the adjacent roadway in the transportation network (i.e., main roads then local roads) and the amount of debris at a collapsed building site (i.e., buildings with large amount of debris first). The amount of debris that can be mobilized between the TAZs and TDMSs using a specific truck in a certain time interval depends on the capacity of the truck and the travel time on the transportation network evaluated by the *post-earthquake traffic* simulator and the loading and unloading times of the debris in and out of the trucks.

The loading and unloading times are assumed to be random variables having a lognormal distribution with median of 1hr. and 0.5 hr., respectively and dispersion of 0.4 for both as per Askarizadeh et al. (2016). The capacity of the truck is assumed to be 18 CY as per Kim et al. (2018). The collected debris is sorted at a TDMS into recyclable and non-recyclable debris. The recyclable percentage of construction debris is assumed to be a random variable with a normal distribution, minimum of 0.05, maximum of 0.15, and mean of 0.08 as per Kim et al. (2018). Excess recyclable debris over the daily recycling rate of TDMSs is mobilized to recycling facilities as shown in Figure 6. A recyclable rate of 4500 CY/day is assumed at each

TDMS as per Kim et al. (2018). The non-recyclable debris is mobilized from TDMS to its final location in landfills (LFs).

MEASURING COMMUNITY PERFORMANCE

The first step to enhance the seismic resilience of a community is to quantify in order to measure the effect of different mitigation strategies on the performance of the community. Several parameters are defined to quantify the performance of both the transportation network and healthcare system.

Transportation Network

The performance of the transportation network is quantified using two parameters: network resilience index (%*NRI*) and network performance index (*NPI*). The network resilience index (%*NRI*) is defined as the area under the recovery path of the transportation network until full recovery (i.e., returning back to 100% functionality) as shown in Figure 9(a) and expressed mathematically as:

$$\%NRI = \frac{\int_0^{T_{NF}} \%Q_{TN}(t)}{T_{NF}} \tag{3}$$

where T_{NF} is the time required for the transportation network to return back to 100% functionality and $\%Q_{TN}(t)$ is the weighted functionality of the transportation network (based on link capacity) at time t during the recovery stage. The weighted functionality of the transportation network is evaluated in the *network recovery* simulator as:

$$\%Q_{TN}(t) = \frac{\sum_{i=1}^{n} C_i \times \%q_i(t)}{\sum_{i=1}^{n} C_i} \tag{4}$$

where n is the number of links in the transportation network, C_i is the traffic flow capacity of link i, and $\%q_i(t)$ is the functionality of link i at time t during the recovery stage which is calculated as:

$$\%q_i(t) = 1 - \%B_i(t) \tag{5}$$

where $\%B_i(t)$ is the percentage blockage of link i at time t during the recovery stage evaluated based on the bridge damage and extent of building debris as described earlier. $\%NRI$ captures the effect of damage and recovery of bridges and buildings on the functionality of the transportation network.

NPI is defined as the area under the mean travel time ratio (*MTTR*) curve of the transportation network as shown in Figure 9(b). Values closer to one suggest that the post-earthquake behavior of the transportation network is close to that experienced before the earthquake. *NPI* captures the effect of building functionality, debris removal trips, and healthcare trips on the O-D demand in the transportation network. It also captures the effect of bridge damage and building debris on the capacity of the links. *NPI* can be expressed mathematically as:

$$NPI = \frac{\int_0^{T_{NP}} MTTR(t)}{T_{NP}} \tag{6}$$

where T_{NP} is the time required to return back to the pre-earthquake travel time on the transportation network and $MTTR(t)$ is the mean travel time ratio of the transportation network at time t during the recovery stage. *MTTR* is defined as the ratio between the weighted mean travel time (*MTT*) on the links of the transportation network in the community at any time t during the recovery stage and the weighted mean travel time on the links of the transportation network before the earthquake (MTT_o) which can be expressed mathematically as:

$$MTTR(t) = \frac{MTT(t)}{MTT_o} \tag{7}$$

$$MTT = \frac{\sum_{i=1}^{n} C_i \times \tau_i}{\sum_{i=1}^{n} C_i} \tag{8}$$

where τ_i is the travel time on link i.

Healthcare System

Three performance parameters are used to quantify the performance of each mechanism in the healthcare system inside the community: hospital utilization index (%*HUI*), in-community mobilization index (%*IMI*) and waiting admission index (%*WAI*). The hospital utilization index (%*HUI*) is defined as the area under the normalized treatment curve of the healthcare system (i.e., normalized number of injuries treated in the hospitals during the recovery stage) as shown in Figure 10(a). A value of 100% means that the hospitals are working at full capacity (i.e., fully utilized) during the recovery stage. %*HUI* can be expressed mathematically as:

$$\%HUI = \frac{\int_0^{T_H} \hat{I}_{TRE}(t)}{T_H} \times 100 \tag{9}$$

where $\hat{I}_{TRE}(t)$ is the number of injuries treated at the hospitals at time *t* during the recovery stage normalized by the capacity of the hospitals in the community at the same time *t*. T_H is the time required to discharge the last injury from the hospitals in the community.

The in-community mobilization index (%*IMI*) is defined as the area under the normalized curve of mobilized injuries inside the community (i.e., normalized number of injuries mobilized from buildings to the hospitals during the recovery stage) as shown in Figure 10(b). A value of 100% suggests that the available ambulances in the community are able to mobilize all of the injuries waiting mobilization during the recovery stage. %*IMI* can be expressed mathematically as:

$$\%IMI = \frac{\int_0^{T_{MI}} \hat{I}_{MI}(t)}{T_{MI}} \times 100 \tag{10}$$

where $\hat{I}_{MI}(t)$ is the number of injuries mobilized inside the community at time *t* during the recovery stage normalized by the number of injuries awaiting mobilization at the same time *t*. T_{MI} is the time required to reach zero injuries mobilized inside the community.

Similar to %*HUI*, the waiting admission index (%*WAI*) is defined as the area under the normalized waiting admission curve of the healthcare system (i.e., normalized number of injuries waiting admission to the hospitals during the recovery stage) as shown in Figure 10(c). A value of 0% suggests that the healthcare system is working efficiently without any injuries waiting admission during the recovery stage. %*WAI* can be expressed mathematically as:

$$\%WAI = \frac{\int_0^{T_{WA}} \hat{I}_{WA}(t)}{T_{WA}} \times 100 \tag{11}$$

where $\hat{I}_{WA}(t)$ is the number of injuries waiting admission to the hospitals at time *t* during the recovery stage normalized by the capacity of the hospitals in the community at the same time *t*. T_{WA} is the time required to reach zero injuries waiting admission to the hospitals.

ILLUSTRATIVE CASE STUDY: SEISMIC RESILIENCE OF ARCHETYPE COMMUNITY

Community Setup

The simulation model and its capabilities are demonstrated through a case study that focuses on modeling the seismic resilience of part of Shelby County, Tennessee (shown in Figure 7). The building portfolio data is the same as per Sediek et al. (2020) which was extracted from the database provided in Ergo-EQ software version 4.0 Beta 2 (NCSA 2018) and mapped to the 100 different archetype buildings developed by Sediek et al. (2020). The studied area is approximately 14 km^2 (5.4 mi^2) with a population of approximately 40,000 (Statistical Atlas 2018) which is considered a typical midsize community. The building portfolio consists of around 8600 buildings, mostly wooden as is typical of US residential communities.

The transportation network data is extracted using the open-source platform OpenStreetMap (OSM) and processed to define the traffic analysis zones (TAZs) using the traffic planning software PTV Visum. Only main roads are modeled in the case study (Figure 7). Local roadways are beyond the scope of this case study. The studied transportation network consists of 306 nodes, 503 links, and 204 TAZs. The traffic demand model used by Memphis MPO (2016) is adopted to predict the trip productions and attractions and

perform modal split for trips with different purposes (i.e., home-based, work-based, etc.) between the different TAZs. Detailed information about the bridges in the studied area is collected from the National Bridge Inventory (NBI 2019), which provides the location of each bridge (Figure 7) and representative values for various bridge parameters required for HAZUS (FEMA 2003) fragility curves.

There are three hospitals in the studied community (Figure 7) that are 2, 4, and 12 stories high with a total number of beds during normal operation of 140, 223, and 326, respectively (Sediek et al. 2020). Braun et al. (1990) reported that cities staff an average of one ambulance per 51,223 people. However, in extreme events as earthquakes this number should be increased. Therefore, it is assumed that 4 ambulances are available in the studied community after the earthquake. This number is an input parameter to the proposed model and can be refined as more data become available from real communities. The rescue rate parameters A and B, defined earlier, are assumed to be 1500 and 1.125 based on a sensitivity study to ensure that all injured are rescued within 24 hours of the earthquake. In real communities, such parameters should be calibrated based on the emergency response capacity of the community. It is also assumed that 10,10, and 5 trucks are available to transport debris from the building sites to TDMS, transport debris from TDMS to the landfill, and transport debris from TDMS to recycling facilities, respectively. It is assumed that two TDMSs, one landfill, and one recycling facility are available and located in the arbitrary locations shown in Figure 7.

Seismic Hazard

The seismic event is the ground motion record RSN 1961 (PEER 2018) which was recorded at the Lepanto station near the studied community to represent the seismic activity in the studied area (Sediek et al. 2020, and Lin and El-Tawil 2020). The epicenter is located at 35°18'N, 90°18'W and the peak ground acceleration (PGA) is scaled at each building location to meet the PGA for a M_w 7.7 earthquake scenario specified by the United States Geological Survey (USGS 2018) for the studied region. The earthquake event is assumed to occur on a weekday at 8:00 PM.

Results and Discussion

To account for the many uncertainties inherent in the factors affecting the behavior of the different systems of the community after a seismic event, the model uses a Monte Carlo procedure to perform loss and recovery calculations. The sampling is performed based on the distribution properties of each component specified in the FEMA P-58 methodology (FEMA 2012) for evaluation of component losses as well as the distribution properties for each variable discussed earlier related to the healthcare system and debris removal. The proposed simulation model is computationally demanding due to the traffic analysis performed at each time step during the recovery stage as well the adopted Monte Carlo procedure. Therefore, the proposed simulation model is implemented and run within a parallel computing environment. The parallelization is performed for the computation of the response and losses of redundant elements of the community in the same realization and time step (e.g., different buildings in the community). A realization in the proposed simulation model represents one Monte Carlo simulation for all the simulators described earlier with a different set of random numbers (i.e., different damage of buildings, losses, etc.). Also, the traffic analysis is performed once every 10 time steps (i.e., 10 days) after the first 30 days as discussed earlier.

The computational time for running a single Monte Carlo realization for the presented case study is approximately 4 hours on a personal computer with four cores and 32 GB RAM. As shown, the proposed simulation model is computationally demanding due to the complex interdependencies inherent between the different simulators. However, it can be used to model larger communities (i.e., city or county level) with some reduction of the resolution of the transportation network (e.g., modeling main roads only in the county) as it is the controlling parameter for the computational cost of the proposed model. The results shown are for one arbitrary Monte Carlo simulation with a constant seed (i.e., same set of random numbers) to be able to demonstrate the capabilities of the proposed model under different conditions (i.e., input

parameters for different scenarios). The complete set of parameters and results of the presented case study are documented and publicly available at Sediek et al. (2021b).

Figure 8 shows the spatial distribution of the traffic flow along the links of the transportation network during the recovery stage immediately after the earthquake and at three other points in time. As shown in Figure 8(a), 55 of the 503 links (~ 11%) in the transportation network lost their functionality (i.e., closed due to debris blockage or bridge damage) immediately after the earthquake. Most of the traffic flow was concentrated around the location of the hospitals due to ambulance trips made to and from hospitals as well as around the location of the landfill and TDMSs due to transportation of debris (Figure 8(a)). The functionality of a significant number of links (i.e., 31 out of 55) was restored within 90 days (i.e., 3 months) of the seismic event as shown in Figure 8(c) due to removal of seismic debris from collapsed buildings and repair of bridges. This progress is also reflected in the recovery trajectory of the transportation network as shown in Figure 9(a) where the functionality of the transportation network increased from 81% immediately after the earthquake to 89% 90 days after the event.

The transportation network was restored to full functionality after 1 year (i.e., 365 days) as shown in Figure 8(d) and Figure 9(a). It should be noted that although the transportation network reached its full functionality, the traffic flow did not return to the pre-earthquake case due to the loss of functionality of some of the buildings. As reported by Sediek et al. (2020), the building portfolio reached its full functionality after 4.6 years which is much longer than the restoration time for the transportation network. The network resilience index (%*NRI*) of the transportation network was 90.5% as shown in Figure 9(a) which is considered acceptable but can be further enhanced. Figure 9(b) shows the mean travel time ratio (*MTTR*) of the studied transportation network during the recovery stage. Immediately after the earthquake, the *MTTR* of the network was 1.3 due to the loss of functionality of the roads as well as the large number of trips made to mobilize injuries and transport debris. However, the *MTTR* of the network dropped significantly during the recovery stage due to the decrease in the trips made as well as the increase in the

network functionality. The network performance index (*NPI*) of the studied network was 1.18 which is close to 1 implying good performance of the network after the seismic event.

Figure 10 shows the evolution of the social functionality (i.e., injured in the community and healthcare system) during the recovery stage. As noted in Figure 10, the time scale is in hours which is different from the time scale of the previous systems (i.e., building portfolio and transportation network). This ability to use multiple time scales is an important capability of the simulation model which allows for different spatial and temporal scales even within the same stage (e.g., recovery stage). As shown in Figure 10(a), the number of treated injuries in the hospitals increased over the first few hours due to mobilization of injuries from the building locations to the hospitals. Eighteen hours after the earthquake, the capacity of the hospitals in the community was reached and the number of injuries waiting admission increased as shown in Figure 10(b). The maximum number of injuries waiting admission was reached after 58 hours from the occurrence of the earthquake as shown in Figure 10(b).

As shown in Figure 10(c), the normalized number of injuries mobilized inside the community was almost constant over the first 24 hours after the earthquake as the number of injuries waiting mobilization was much more than the capacity of the ambulances due to the continuous rescue of the injured. However, after 24 hours, rescue of those injured stopped but the mobilization of the injured continued causing the sharp increase shown in Figure 10(c) until reaching a value of 1 (i.e., all the injuries waiting mobilization are mobilized). The time required to reach zero injuries (i.e., treat all who were injured) was 270 hours (~11 days). As shown in Figure 10, %*HUI*, %*IMI,* and %*WAI* were 51%, 15%, and 50% respectively.

Impact of Interdependencies

The proposed simulation model shown in Figure 2 was modified to study the effect of removing or adding interdependencies between the different systems by simply removing or adding the connection (shown by the arrows connecting the boxes in Figure 2) between the relevant simulators. Two types of

interdependencies were studied: those between the *post-earthquake traffic* simulator and the *debris removal* simulator, and *healthcare* simulator. The first interdependency considers the effect of building debris (related to building portfolio) on the functionality of the links in the transportation network. The lack of considering the second interdependency means that the healthcare system is not affected (i.e., constrained) by the functionality of the transportation network. In this case, all the injured who are rescued are assumed to be mobilized in one time step with no constraint on the number of trips that can be made through the transportation network. This assumption is made by most of the studies available in the literature (e.g., Ceferino et al. 2020).

Figure 11(a) shows the recovery trajectory of the studied transportation network with and without considering the first interdependency. Considering the interdependency between the *post-earthquake traffic* and *debris removal* simulators (indexed as "bridge only" in Figure 11(a)) had two effects on the recovery trajectory of the transportation network. First, it shifted the recovery trajectory to the right (green shaded area in Figure 11(a)) due to the time required to remove the debris from the partially and totally blocked links. The second effect was to reduce the initial post-earthquake functionality of the network from 90% to 81% (9% reduction) due to the partial and total blockage of the links affected by the debris resulting from the collapse of the buildings.

Figure 11(b) shows the effect of the interdependency between *post-earthquake traffic* and *healthcare* simulators on the performance of the healthcare system through % *HUI*, %*WAI*, and %*IMI*. As shown, neglecting the interdependency between *post-earthquake traffic* and *healthcare* simulators had a significant effect on %*IMI* which increased from 15% to 100%. This result is attributed to the assumption that there was no constraint on the number of injured that can be mobilized to the hospitals in the community at any time step. This effect is also reflected in %*HUI* and %*WAI* which increased from 51% to 64% and from 50% to 98%, respectively, for the same reason. As shown, the novel approach implemented to consider the mutual interdependency between the transportation network and healthcare system in the community has a

significant effect (i.e., more realistic) on the predicted behavior of the healthcare system in the community. This approach enables a better understanding of how these systems will function and an improved ability to enhance the behavior of these two systems after seismic events.

Effectiveness of Hazard Mitigation Plans

The capability of the simulation model to support decision makers in studying the effect of different mitigation actions on the behavior of the studied systems (i.e., healthcare, building portfolio, and transportation network) is demonstrated through a sensitivity study that comprises different mitigation actions. For the healthcare system, the studied mitigation action entailed three activities. The first activity was increasing the number of ambulances available after the earthquake from 4 to 8. The second activity was adding a field hospital near to the 12-story hospital (i.e., the same TAZ) with an additional 180 beds. The third activity was enhancing the emergency response of the rescue team in the community after the earthquake (e.g., receiving supporting rescue personnel from nearby zones or states) by changing the rescue rate parameters A and B defined earlier from 1500 to 2000 and from 1.15 to 1.1, respectively.

For the building portfolio, the mitigation action entailed a community-wide building retrofit plan to upgrade the seismic resistance of all buildings that were built according to design codes prior to 1973 to meet current design requirements. For debris removal mitigation action, the number of trucks available to collect debris from the building sites and transport it to TDMS and to transport debris from TDMS to the landfill was increased to 20. The number of TDMSs available in the community was increased to 3 with the same assumed capacity per TDM (i.e., 30,000 CY). All possible combinations of these three mitigation strategies were considered leading to eight different scenarios as defined in Table 3. It should be noted that these mitigation actions are for the purpose of demonstrating the capabilities of the proposed simulation model only and that no mitigation decisions can be made based on a single case and a single event without taking into account the uncertainties. More work is required to have valid quantitative mitigation plans and one case is not sufficient for such purpose.

Figure 12 shows the effect that the mitigation actions related to debris removal and the building portfolio had on the transportation network. As shown in Figure 12(a), upgrading the seismic design of the buildings in the community led to an increase in the initial functionality of the transportation network from 81% to 90% (9% increase) which is attributed to the lower number of collapsed buildings (mainly RC and steel buildings). This increase in initial functionality is also reflected in the initial *MTTR* after the earthquake which decreased from 1.30 to 1.05 (20% reduction) as shown in Figure 12(b), *NPI* which decreased from 1.18 to 1.02 (14% reduction), and %*NRI* which increased from 90.5% to 95% (5% increase). The mitigation actions related to debris removal shifted the recovery trajectory of the transportation network to the left due to the expedited clearance of the roadways as shown in Figure 12(a). This outcome is also reflected in %*NRI* which increased from 90.5% to 92% (1.5% increase), and *NPI* which decreased from 1.18 to 1.1 (7% reduction).

Figure 13 shows the effect that the mitigation actions related to the healthcare system and the building portfolio had on the number of injured waiting admission to hospitals as well as the number of injured being mobilized. As shown in Figure 13(a), the proposed mitigation actions had a significant effect on %*WAI* which decreased from 50% to 12% (76% reduction) due to the increased number of available beds in the community. Also, the number of fatalities in the community significantly decreased from 384 to 278 due to the reduced number of collapsed buildings in the community resulting from the seismic design upgrade. Upgrading the seismic design of buildings along with the mitigation actions for the healthcare system had the most significant effect on %*WAI* which decreased from 50% to almost 0 (1% as shown in Figure 13(a)) due to both the increased number of available beds as well as reduced number of collapsed buildings in the community. Also, these two mitigation strategies had a significant effect on the number of fatalities in the community which decreased from 384 to 127 for the same reasons.

Increasing the number of ambulances as well as enhancing the emergency response of the rescue team in the community had a significant effect on the time required to mobilize all the injuries waiting mobilization in the community which decreased from 65 to 38 hours (42% reduction) as shown in Figure 13(b). Upgrading the seismic design of the buildings had a similar effect, due to the reduced number of injured resulting from collapsed buildings, where the time required to mobilize all the injuries waiting mobilization in the community decreased from 65 to 45 hours (30% reduction).

Choosing the appropriate mitigation strategy depends on many factors which are community specific beyond just the performance parameters discussed earlier (e.g., %*NRI*, *NPI*, %*WAI*, %*IMI*, etc.). One of these factors is the initial investment required for each plan (e.g., the cost of upgrading the design of current buildings versus repairing them after a seismic event). Another factor is the social aspect of the problem. For example, the mitigation actions related to the healthcare systems may have a significant economic cost. However, the social gain from such mitigation actions (i.e., reducing number of fatalities or number of injuries mobilized outside the community) may be much higher than the economic cost. As demonstrated, the proposed simulation model can be used by decision makers in the community to make such tradeoffs and decide on viable mitigation strategies to be executed.

SIMULATION MODEL LIMITATIONS

Although the proposed simulation model considers the interdependencies between the building portfolio, transportation network and healthcare system during and after seismic events, there are still other critical dimensions of community resilience that have not been accounted for in this study. Damage and recovery of lifeline systems is one of these critical dimensions which deeply influence resilience and the recovery trajectory. Also, social losses are only expressed in terms of casualties, which is not the case in real communities where other short- and long-term social vulnerability indicators affect the resilience of communities including relocation, business disruption, job loss, supply disruption, family stress and neighborhood disruption that are outside the scope of this study. For example, shortage of medical staff in

hospitals is assumed to be because of casualties only in the proposed simulation model. However, other reasons may also cause this shortage such as injury of a family member of the staff, or their relocation to other cities, etc. All of these dimensions can be added to the proposed model with the addition of appropriate simulators and their connection with the rest of the system model shown in Figure 2.

Also, the presented results and mitigation strategies are based on the assumptions discussed earlier related to the building portfolio, transportation network, and healthcare system. Clearly, the results (i.e., building collapse, injuries and recovery outcomes) will change when using different input parameters. However, the proposed model allows for the ability to evaluate multiple scenarios and strategies taking into consideration the effect of interdependencies between the three critical systems discussed earlier which provides the necessary data to make informed decisions. Another limitation is that the shown results and mitigation strategies are based on only one Monte Carlo simulation which does not necessarily represent the big picture statistically, because other random realizations may give different results. However, the proposed model allows for the ability to evaluate multiple Monte Carlo realizations for multiple scenarios conditioned upon the availability of required computational resources. Also, a lot of the parameters discussed earlier that are adopted from other studies that are not originally developed for the studied region. This is attributed to the lack of the availability of the data in the studied region.

SUMMARY AND CONCLUSIONS

A simulation-based model is presented for the assessment and quantification of seismic resilience of communities while considering the mutual interdependencies between the building portfolio, transportation network, and healthcare system. The model was modularized into independent simulators, each representing an aspect of the overall problem to facilitate modeling such complex interdependencies. The proposed model combined the effect of bridge damage and accumulation of debris resulting from the collapsed buildings on the transportation network. The post-disaster origin-destination (O-D) patterns of households along with the functionality of the road network were used in a traffic analysis to update the

traffic flow and time through the links of the transportation network. The updated traffic flow and time were used in a discrete event simulation (DES) environment to simulate the behavior of the healthcare system as well as the debris removal process in the aftermath of a seismic event.

Resilience measures for each system were proposed to assess and improve the seismic resilience of the individual systems and the community as a whole. The model was demonstrated through a case study in which the building portfolio, transportation network, and healthcare system of a part of Shelby County, Tennessee, was subjected to a M_w 7.7 earthquake located northwest of Memphis. The results of one realization showed that 11% of the links in the studied transportation network lost their functionality due to debris accumulation and bridge damage which adversely affected the mobilization of injured people as well as debris removal from the community. In order to demonstrate the capability of the simulation model to support hazard mitigation planning, a sensitivity study was performed to investigate the effect of three mitigation actions related to the three studied systems (i.e., healthcare, building portfolio, and debris removal). All possible combinations between the three mitigation actions were considered leading to eight different scenarios. The results of the case study showed that upgrading the seismic design of buildings and increasing the number of ambulances and hospital beds in the community reduced the number of fatalities by 50%. Also, upgrading the seismic design of buildings and increasing the number of trucks used to transport debris in the community improved the seismic resilience of the transportation network by 5%.

The proposed simulation model is a key step forward towards quantifying and enhancing the seismic resilience of communities while considering the mutual interdependencies between the different critical systems in a community. Choosing the appropriate mitigation strategy to improve the seismic resilience of a community is a challenging task that depends on many factors beyond just the economic cost. For example, the mitigation actions required for the healthcare systems may have a significant economic cost. However, the social gain from such mitigation actions (i.e., reducing number of fatalities or number of injuries mobilized outside the community) may be much higher than the economic cost. The simulation model can

be used by decision makers in the community to make such tradeoffs and decide on viable mitigation strategies to be executed.

DATA AVAILABILITY STATEMENT

Some or all data, models, or code generated or used during the study are available in a repository online in accordance with funder data retention policies. (https://doi.org/10.17603/ds2-m3b2-re28)

ACKNOWLEDGEMENTS

This work was supported by the University of Michigan and the US National Science Foundation (NSF) through grant ACI-1638186. Any opinions, findings, conclusions, and recommendations expressed in this paper are those of the authors and do not necessarily reflect the views of the sponsors.

REFERENCES

Alvanchi, A., Lee, S. H., and AbouRizk, S. (2011). "Modeling Framework and Architecture of Hybrid System Dynamics and Discrete Event Simulation for Construction." *Computer-Aided Civil and Infrastructure Engineering*, 26(2), 77–91.

Argyroudis, S., Selva, J., Gehl, P., and Pitilakis, K., 2015. "Systemic seismic risk assessment of road networks considering interactions with the built environment." *Computer-Aided Civil and Infrastructure Engineering* 30, 524–540.

Askarizadeh, L., Karbassi, A. R., Ghalibaf, M. B., and Nouri, J. (2016). "Management of post-earthquake construction debris in Tehran Metropolitan." *International Journal of Environmental Science and Technology*, 13(2), 639–648.

Biggs, N. L., Lloyd , E. K. and Wilson ,R. J. (1986) *Graph Theory* 1736-1936, 2nd edn, Oxford

Braun, O., McCallion, R., & Fazackerley, J. (1990). "Characteristics of midsized urban EMS systems." *Annals of Emergency Medicine*, 19(5), 536–546.

Bruycker, M., Greco, D., Annino, I., Stazi, M. A., de Ruggiero, N., Triassi, M., de Kettenis, Y. P., and Lechat, M. F. (1983). "The 1980 earthquake in southern Italy: Rescue of trapped victims and mortality." *Bulletin of the World Health Organization*, 61(6), 1021–1025.

Burton, H. V., Deierlein, G., Lallemant, D., and Singh, Y. (2017). "Measuring the Impact of Enhanced Building Performance on the Seismic Resilience of a Residential Community," *Earthquake Spectra*, 33(4), 1347–1367.

Castro, S., Poulos, A., and Herrera, C. (2019). "Modeling the Impact of Earthquake- Induced Debris on Tsunami Evacuation Times of Coastal Cities." *Earthquake Spectra.* 35(1), 137–158.

Ceferino, L., Mitrani-Reiser, J., Kiremidjian, A., Deierlein, G., and Bambarén, C. (2020). "Effective plans for hospital system response to earthquake emergencies." *Nature Communications*, 11(1)

Cigolini, R., Pero, M., Rossi, T., and Sianesi, A. (2014). "Linking supply chain configuration to supply chain perfrmance: A discrete event simulation model." *Simulation Modelling Practice and Theory*, 40, 1–11.

Cimellaro, G. P., Arcidiacono, V., Reinhorn, A. M., and Bruneau, M. (2013). "Disaster resilience of hospitals considering emergency ambulance services." *Proceedings of the 2013 Structures Congress*, 2824–2836.

Coupland, R.M. (1994). "Epidemiological Approach to Surgical Management of the Casualties of War." *British Medical Journal* 308: 1693–6.

Domaneschi, M., Paolo, G., and Scutiero, G. (2019). "A simplified method to assess generation of seismic debris for masonry structures." *Engineering Structures*, 186 (December 2018), 306–320.

Evans, S. P. (1976). "Derivation and analysis of some models for combining trip distribution and assignment." *Transportation Research*, 10, 37-57

Fawcett, W., and Oliveira, C. S. (2000). "Casualty treatment after earthquake disasters: Development of a regional simulation model." *Disasters*, 24(3), 271–287.

Fu, Z., Gao, R. and Yiming, L. (2021). "Measuring seismic resilience of building portfolios based on innovative damage ratio assessment model." *Structures*, 30(4), 1109–1126.

FEMA (2003). "Earthquake loss estimation methodology: Technical manual." *National Institute of Building for the Federal Emergency Management Agency*, Washington, DC.

FEMA (2007). "Public Assistance: Debris Management Guide", *National Institute of Building for the Federal Emergency Management Agency*, Washington, DC.

FEMA (2010). "Debris Estimating Field Guide." FEMA 329, *Federal Emergency Management Agency*, Washington, DC.

FEMA. (2012). "Seismic performance assessment of buildings. FEMA P58-1" *Applied Technology Council*, Redwood City, CA.

Feng, K., Li, Q., and Ellingwood, B. R. (2020). "Post-earthquake modelling of transportation networks using an agent-based model." *Structure and Infrastructure Engineering*, 16(11), 1578–1592.

Gentile, R., and Galasso, C. (2020). "Gaussian process regression for seismic fragility assessment of building portfolios." *Structural Safety*, 87(11), 101980.

Hamrock, E., Paige, K., Parks, J., Scheulen, J., and Levin, S. (2013). "Discrete event simulation for healthcare organizations: A tool for decision making." *Journal of Healthcare Management*, 58(2), 110–124.

Hasan, I., Bahalkeh, E., and Yih, Y. (2020). "Evaluating intensive care unit admission and discharge policies using a discrete event simulation model." *Simulation*, 96(6), 501–518.

Hassan, E. M., and Mahmoud, H. (2020) "An integrated socio-technical approach for post-earthquake recovery of interdependent healthcare system." *Reliab. Eng. Syst. Saf.* doi:10.1016/j.ress.2020.106953.

Hirokawa, N., and Osaragi, T. (2015). "Earthquake Disaster Simulation System : Integration of Models for Building Collapse , Road Blockage , and Fire Spread" *Journal of Disaster Research* Vol.11 No.2, 2016.

Isard, W. (Ed.). (1956). *Location and space-economy*. The MIT Press: London, England.

Jun, J. B., Jacobson, S. H., and Swisher, J. R. (1999). "Application of discrete-event simulation in health care clinics: A survey." *Journal of the Operational Research Society*, 50(2), 109–123.

Kim, J., Deshmukh, A., and Hastak, M. (2018). "A framework for assessing the resilience of a disaster debris management system." *International Journal of Disaster Risk Reduction*, 28(January), 674–687.

Kirsch TD, Mitrani-Reiser J, Bissell R, Sauer LM, Mahoney M, Holmes WT, Santa Cruz N, and de la Maza F. (2010), "Impact on hospital functions following the 2010 Chilean earthquake." *Disaster Med Public Health Prep*. 2010 Jun;4(2):122-8.

Lin, S. Y., and El-Tawil, S. (2020). "Time-dependent resilience assessment of seismic damage and restoration of interdependent lifeline systems." *Journal of Infrastructure Systems*, 26(1), 04019040. doi:10.1061/(ASCE)IS.1943-555X.0000522

Memphis Metropolitan Planning Organization (MPO). (2016). "Travel Demand Model Documentation. Livability 2040: Regional Transportation Plan" Appendix B.

Mitrani-Reiser, J., Mahoney, M., Holmes, W. T., de la Llera, J. C., Bissell, R., and and Kirsch, T., (2012), "A functional loss assessment of a hospital system in the Bío-Bío province." *Earthquake Spectra* 28, 473–502.

Mulvey, J. M., Awan, S. U., Qadri, A. A., and Maqsood, M. A. (2008). "Profile of injuries arising from the 2005 Kashmir Earthquake: The first 72 h." *Injury*, 39(5), 554–560.

NBI (2019). ⟨ https://www.fhwa.dot.gov/bridge/nbi/ascii2019.cfm ⟩ *National Bridge Inventory* (Apr. 15, 2020).

NCSA (2018). "ERGO-EQ Platform for Multi-Hazard Assessment, Response, and Planning." *National Center for Supercomputing Applications and Mid America Earthquake Center*, < http://ergo.ncsa.illinois.edu/?page_id=44>, (accessed August 2018).

Padgett, J.E. and DesRoches, R. (2007). "Bridge functionality relationships for improved seismic risk assessment of transportation networks." *Earthquake Spectra*, 23, 115– 30.

PEER (2018). "PEER Ground Motion Database." *Pacific Earthquake Engineering Research Center* <https://ngawest2.berkeley.edu/> (Accessed Aug. 2018).

Phalkey, R., Reinhardt, J. D., and Marx, M. (2011). "Injury epidemiology after the 2001 Gujarat earthquake in India: a retrospective analysis of injuries treated at a rural hospital in the Kutch district immediately after the disaster." *Global Health Action*, 4, 7196.

Robinson, S. (2004). "*Simulation – The practice of model development and use*." Wiley.

Sediek, O. A, El-Tawil, S. and McCormick, J. (2020), "Dynamic Modeling of In-Event Interdependencies in Community Resilience," *Natural Hazards Review*, 21 (4), 04020041.

Sediek, O. A, El-Tawil, S. and McCormick, J. (2021a), "Seismic Debris Field for Collapsed RC Moment Resisting Frame Buildings," Accepted for publication in *J. Struct. Eng.*

Sediek, O. A, El-Tawil, S. and McCormick, J. (2021b), "A Case Study for Modeling Interdependencies Between the Building Portfolio, Transportation Network, and Healthcare System in the Community," DesignSafe-CI. DOI: 10.17603/ds2-m3b2-re28

Shiraki, N., Shinozuka, M., Moore, J. E., Chang, S. E., Kameda, H., and Tanaka, S. (2007). "System risk curves: Probabilistic performance scenarios for highway networks subject to earthquake damage." *J. Infrastruct. Syst*.

Statistical Atlas (2018). "Population of Shelby County, Tennessee." *Educational Attainment in the United States - Statistical Atlas.*

Somy, S., Shafaei, R., and Ramezanian, R. (2021). "Resilience-based mathematical model to restore disrupted road-bridge transportation networks." *Structure and Infrastructure Engineering,* DOI: 10.1080/15732479.2021.1906711

Su, Y., Yang, L., and Jin, Z., (2008). "Simulation and system dynamics models for transportation of patients following a disaster." *Proceedings of* 2008 *International Workshop on Modelling, Simulation and Optimization*, WMSO 2008, 93–96.

USGS (2018). "Memphis, Shelby County Seismic Hazard Maps and Data Download". *The United States Geological Survey* https://earthquake.usgs.gov/hazards/urban/memphis/grid_download.php>, (Accessed Aug. 2018).

Vishnu, N., Kameshwar, S., and Padgett, J. E. (2018). "A framework for resilience assessment of highway transportation networks." *Routledge Handbook of Sustainable and Resilient Infrastructure*, 1, 216–238.

Wardrop, J. (1952). "Some Theoretical Aspects of Road Traffic Research." *Proceedings of the Institute of Civil Engineers, Part II,* 1, 325-378.

Weiner,E. (1997). U*rban Transportation Planning in the United States: An Historical Overview* (fifth edition), Report DOT-T-97-24, US Department of Transportation, Washington, DC

Zhang, X., Mahadevan, S., and Goebel, K. (2019). "Network Reconfiguration for Increasing Transportation System Resilience Under Extreme Events." *Risk Analysis*, 39(9), 2054–2075.

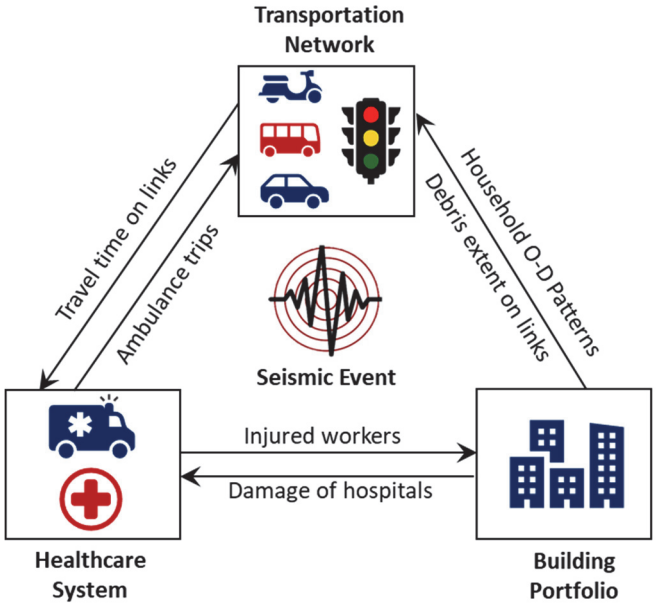

Figure 1: Interdependencies between community sectors

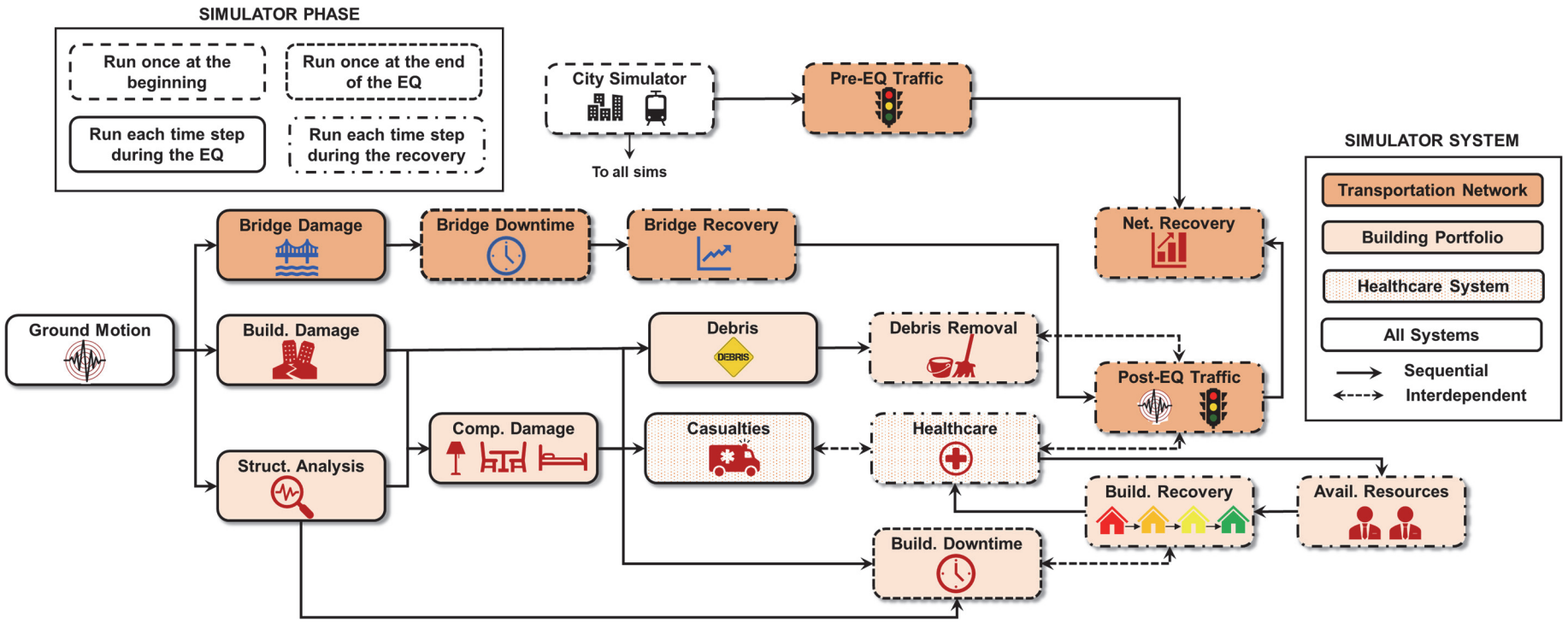

Figure 2: Simulation model overview

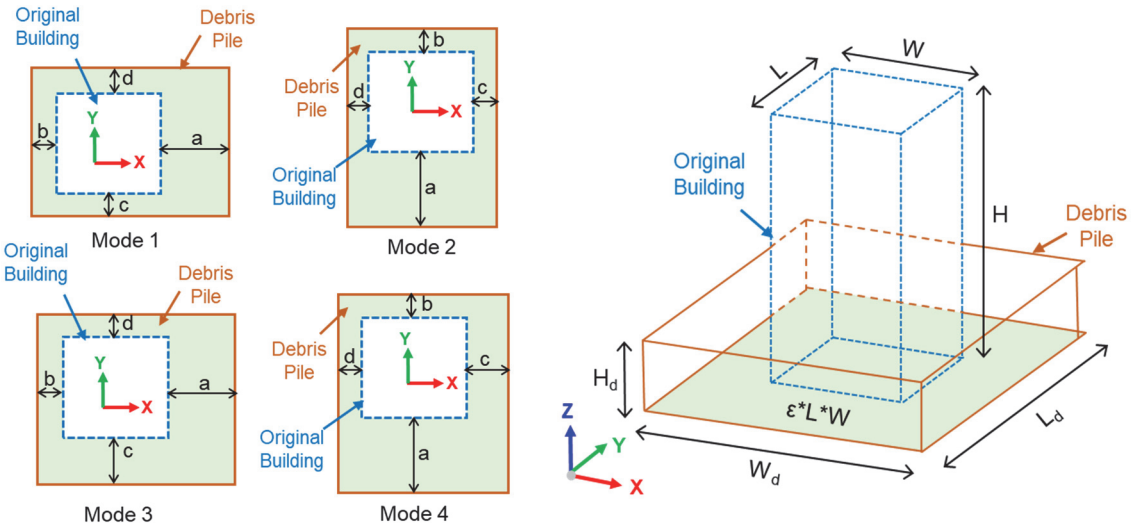

Figure 3: Assumed shape of seismic debris pile resulting from the collapse of: (a) RC frame; (b) masonry; and (c) other types of buildings in the community.

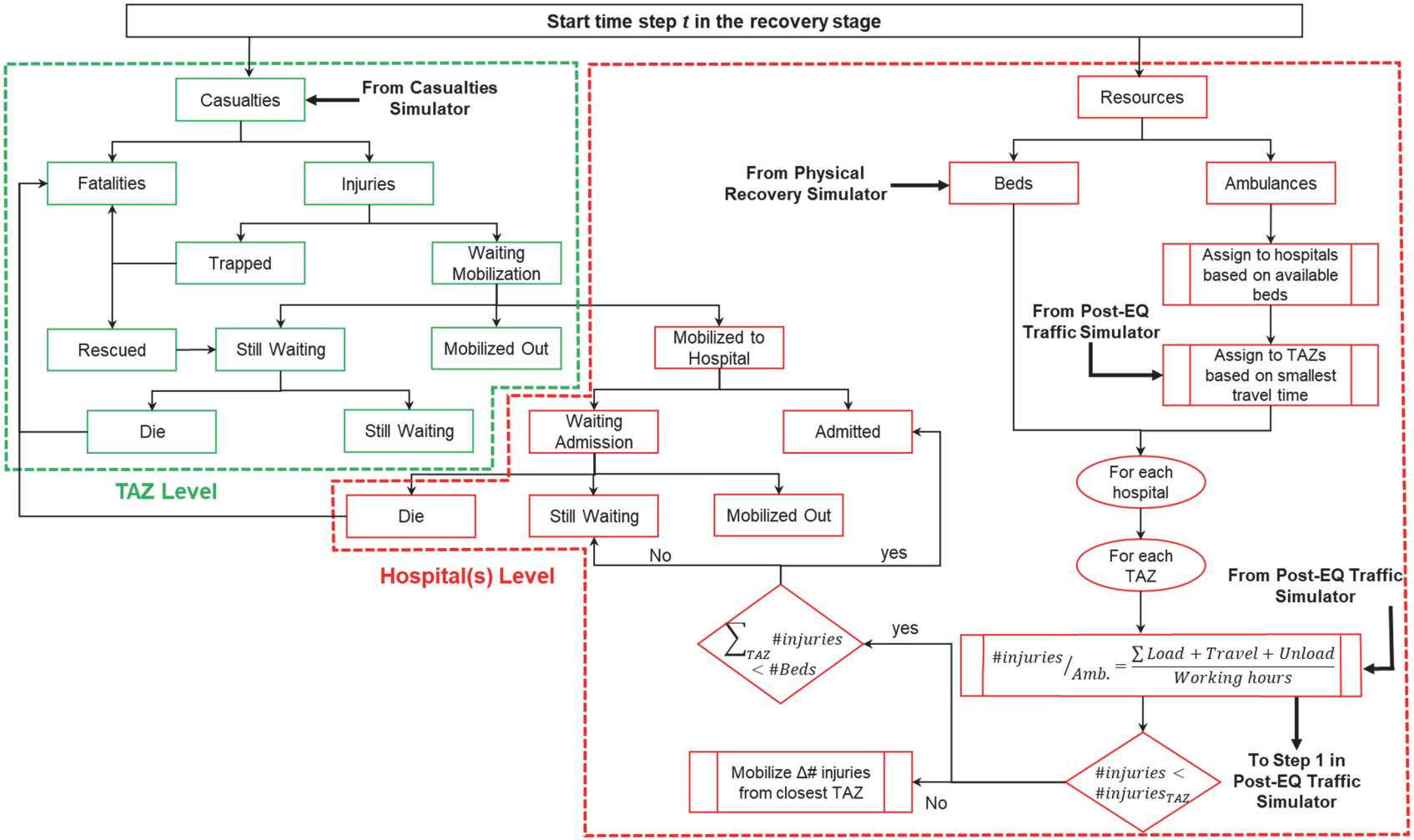

Figure 4: Overview of DES implemented in *healthcare* simulator

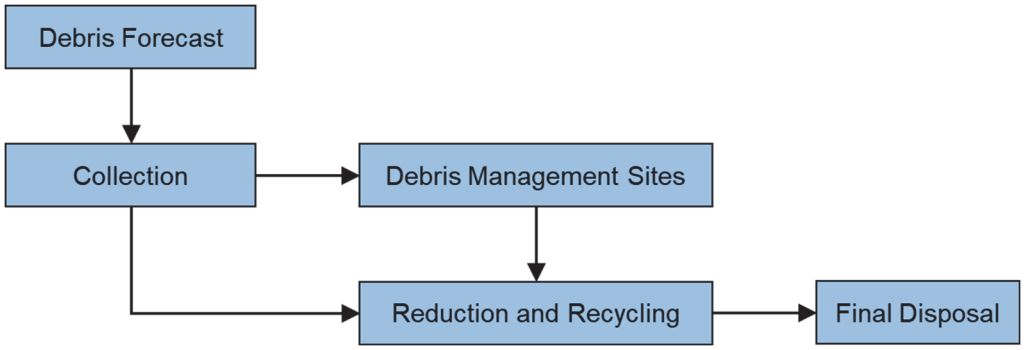

Figure 5: Debris removal process outlined in FEMA-325 (2007)

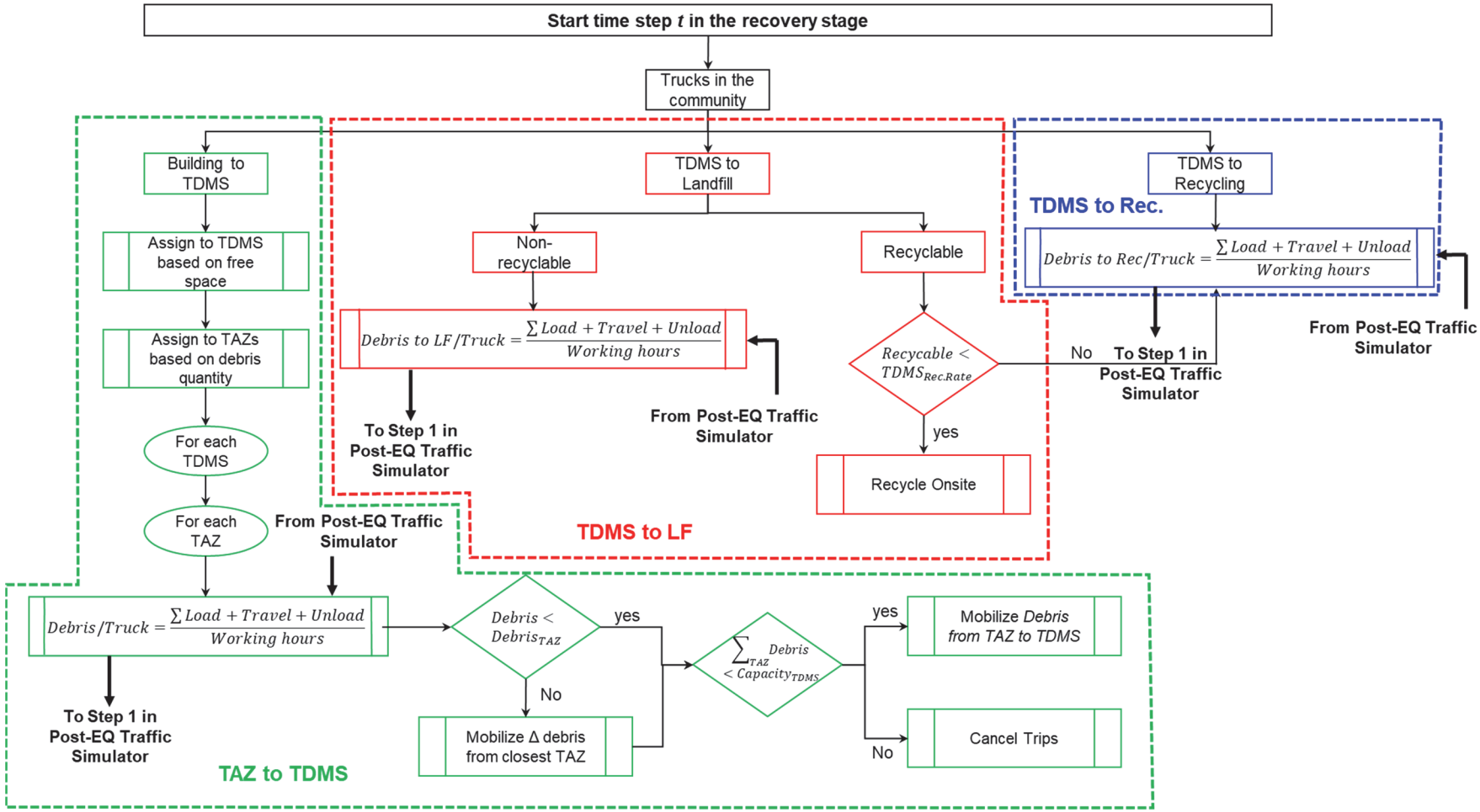

Figure 6: Overview of DES implemented in *debris removal* simulator

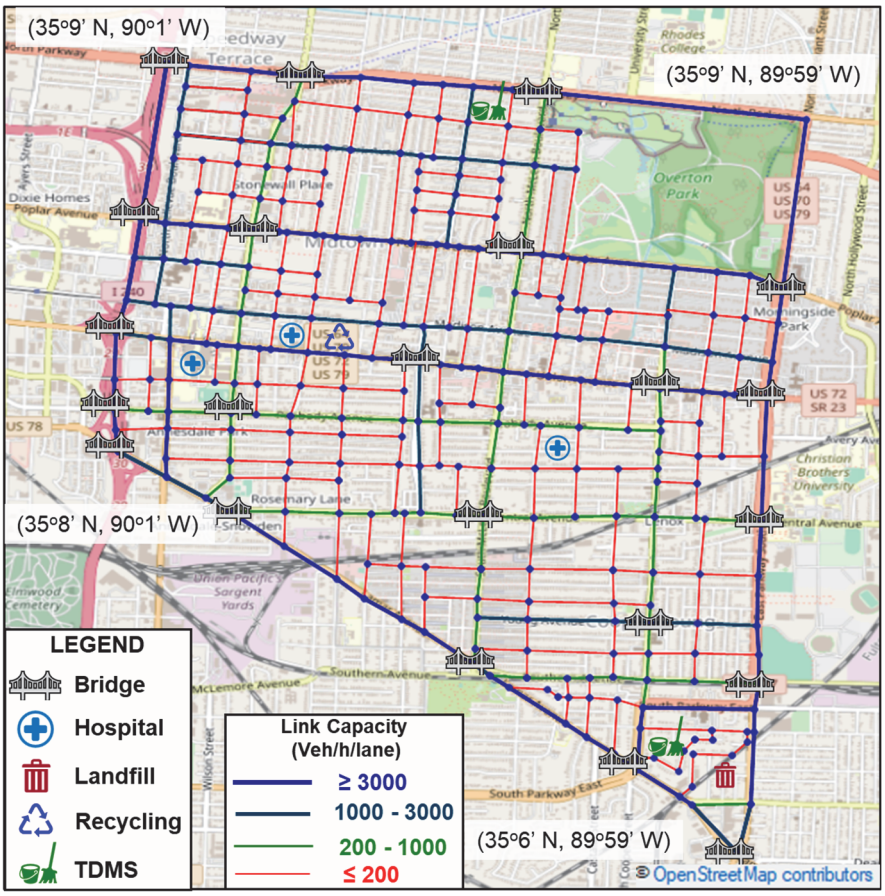

Figure 7: Studied community

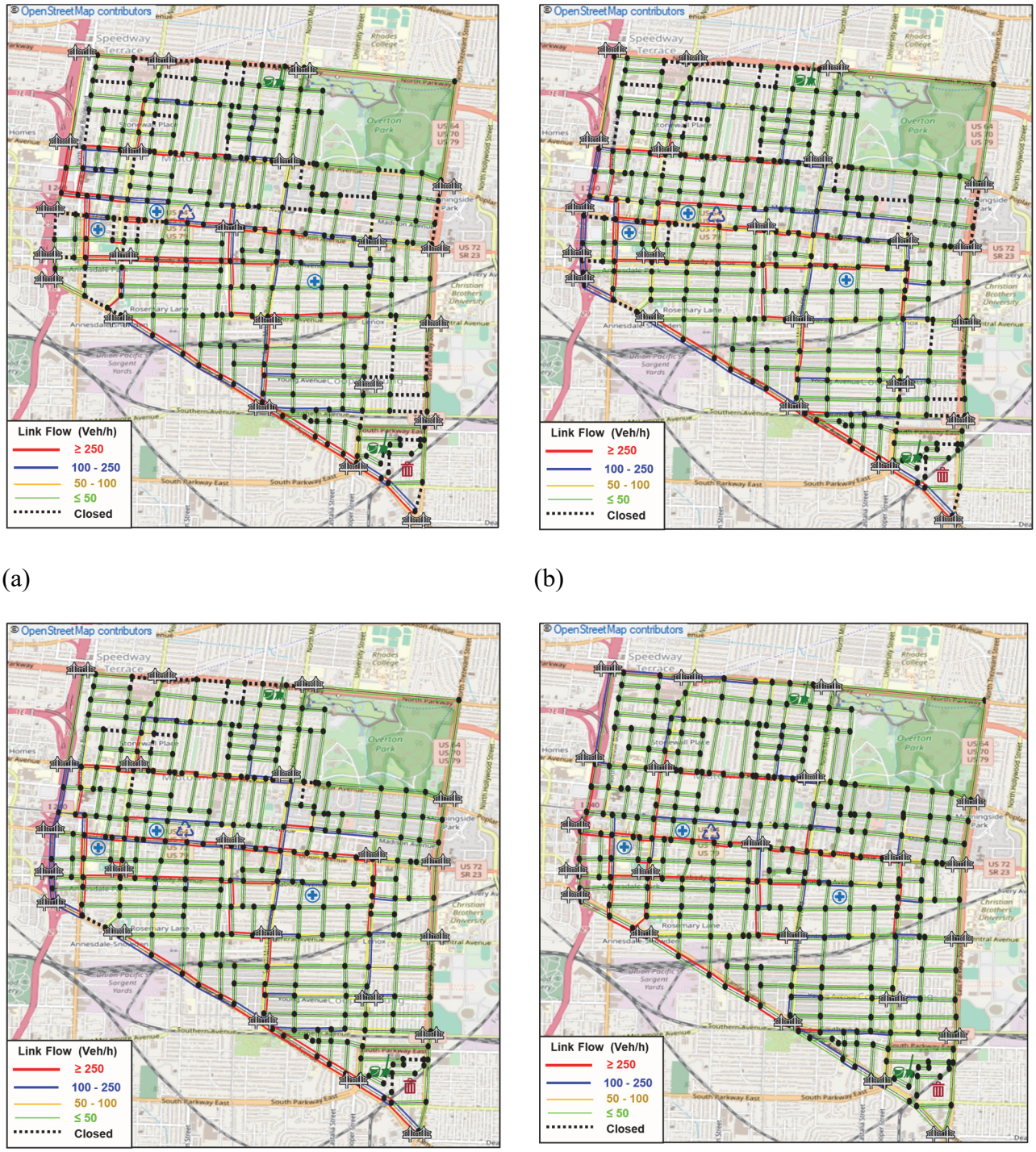

Figure 8: Spatial distribution of link flow in the transportation network for one arbitrary Monte Carlo simulation: (a) immediately after the earthquake; (b) after 1 month; (c) after 3 months; and (d) after 12 months

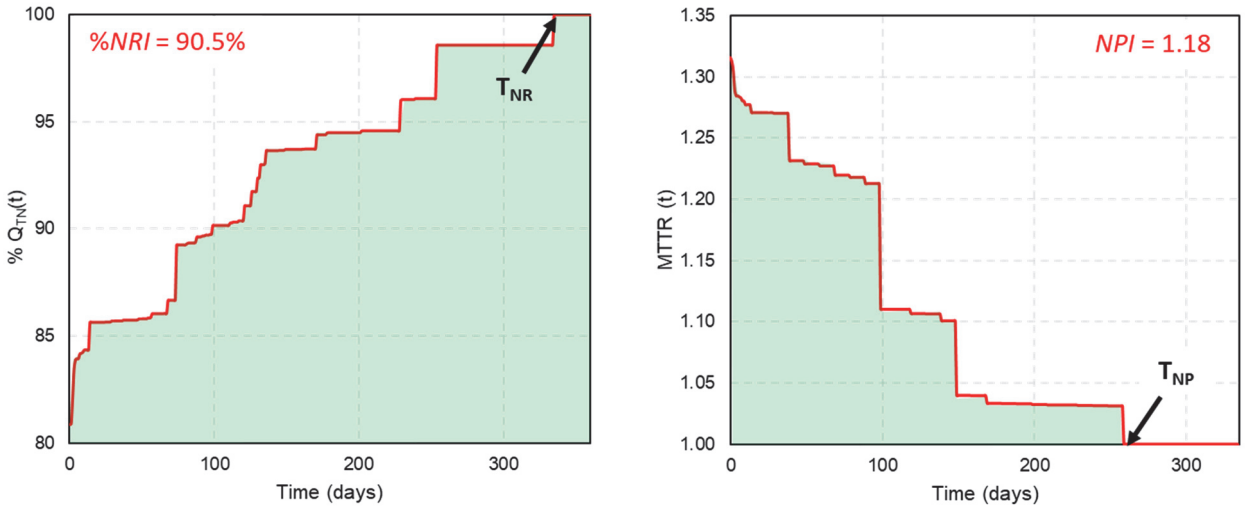

(a) (b)

Figure 9: Illustration of: (a) recovery trajectory of the transportation network after the earthquake for one arbitrary Monte Carlo simulation; and (b) mean travel time ratio (MTTR) of the studied network during the recovery stage

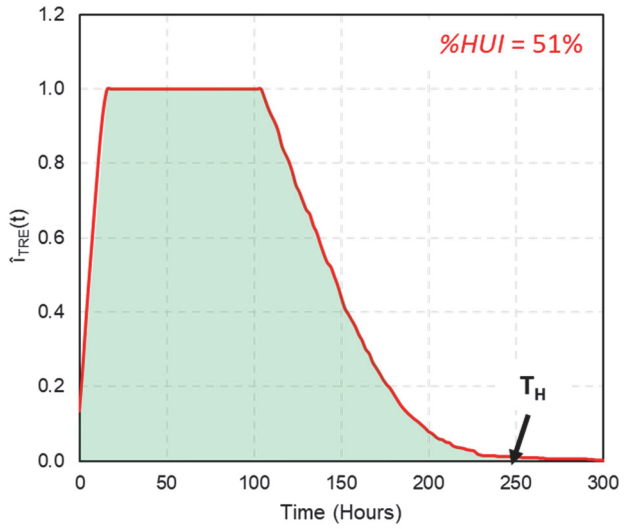

(a)

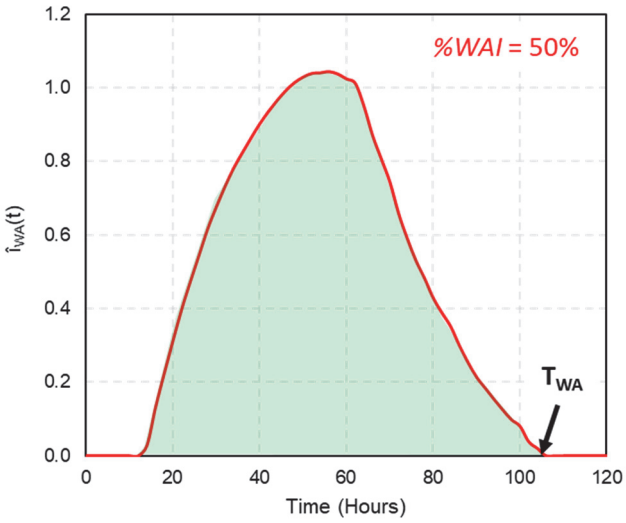

(b)

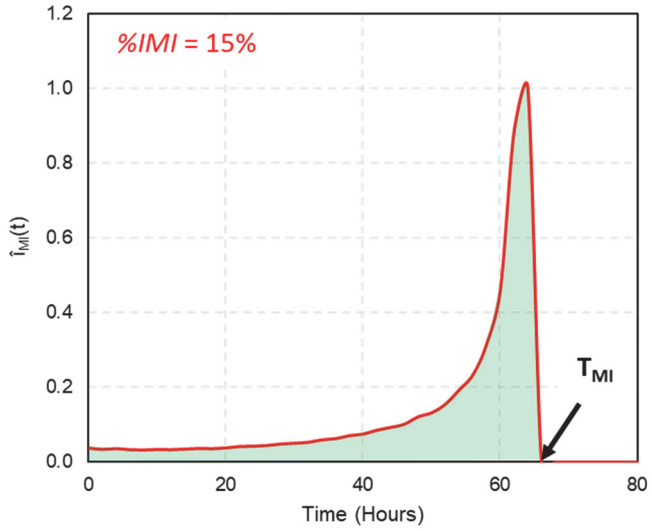

(c)

Figure 10: Illustration of number of injuries for one arbitrary Monte Carlo simulation: (a) receiving treatment in in the hospitals; (b) mobilized between building locations and the hospitals during the recovery stage; and (c) awaiting admission to the hospitals during the recovery stage

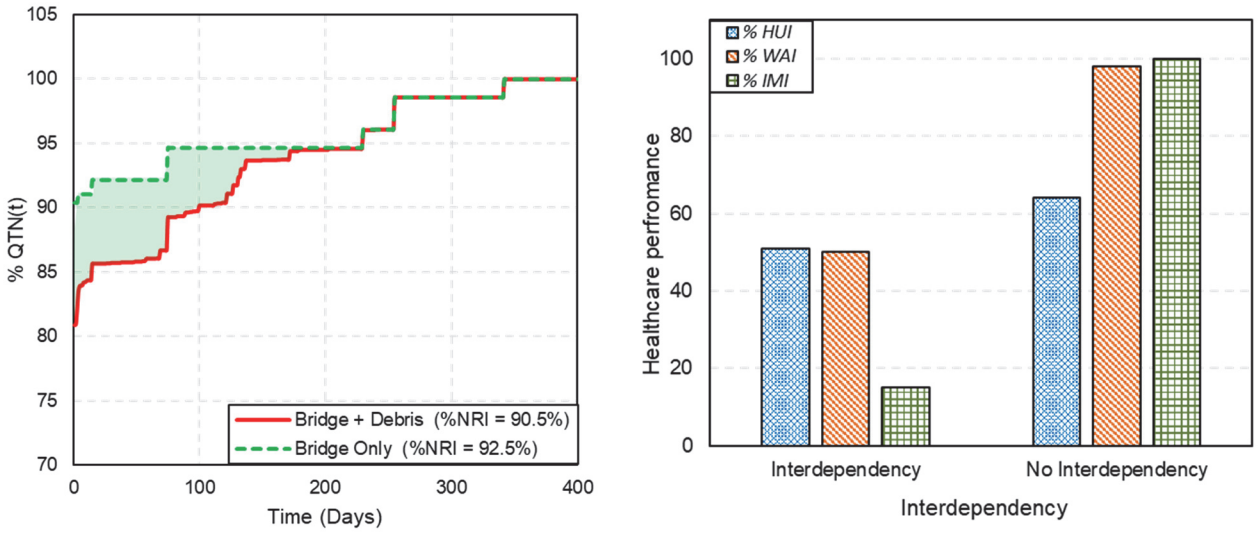

(a) (b)

Figure 11: Effect of interdependencies between: (a) *post-earthquake traffic* simulator and *debris removal* simulator; and (b) *post-earthquake traffic* simulator and *healthcare* simulator

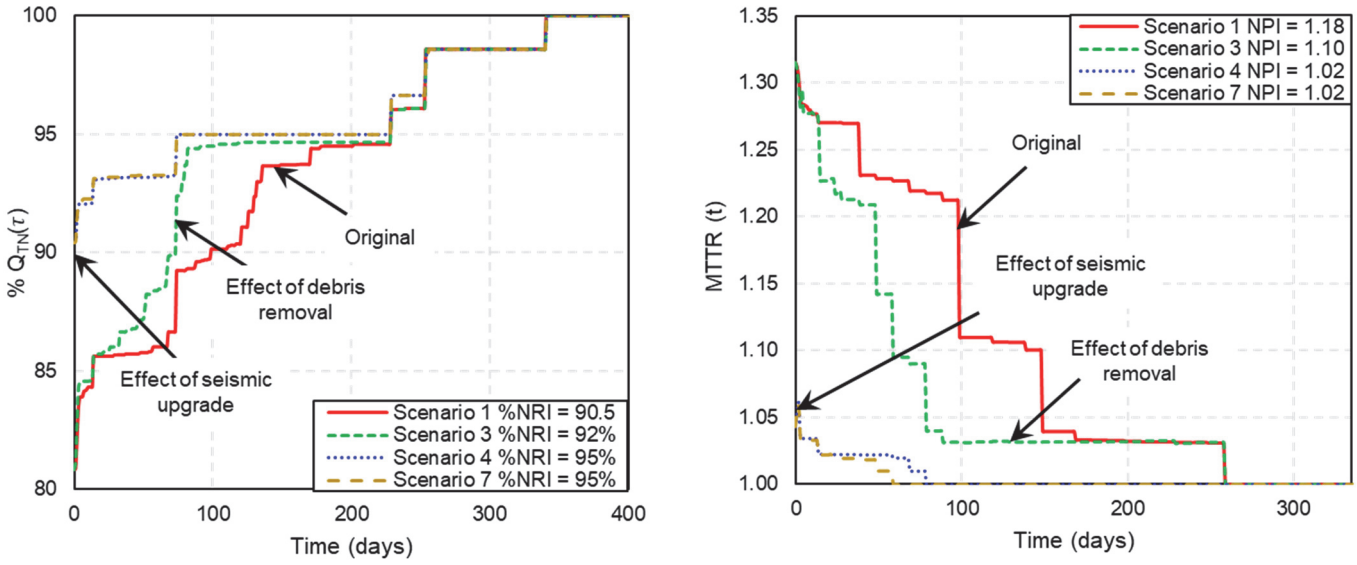

(a) (b)

Figure 12: Effect of studied mitigation strategies on: (a) transportation network recovery trajectory, and (b) mean travel time ratio (*MTTR*)

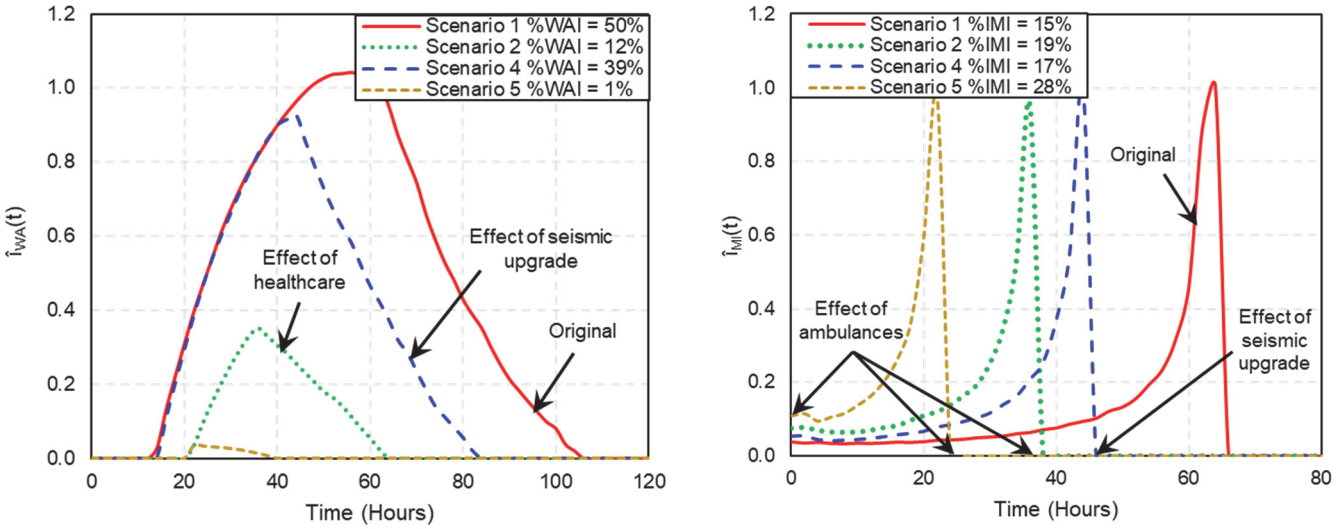

(a) (b)

Figure 13: Effect of studied mitigation strategies on: (a) number of injuries waiting admission to hospitals, and (b) number of injuries mobilized.